Respiratory-driven Cyclic Cerebrospinal Fluid Motion in the Intracranial Cavity on Magnetic Resonance Imaging: Insights into the Pathophysiology of Neurofluid Dysfunction

Yumetaro SAKAKIBARA,[1] Satoshi YATSUSHIRO,[2] Natsuo KONTA,[3,4]
Tomohiko HORIE,[3] Kagayaki KURODA,[5] and Mitsunori MATSUMAE[1]

[1]Department of Neurosurgery, Tokai University School of Medicine, Isehara, Kanagawa, Japan
[2]BioView Inc., Tokyo, Japan
[3]Department of Radiology, Tokai University School of Medicine, Isehara, Kanagawa, Japan
[4]Graduate School of Radiological Technology, Gunma Prefectural College of Health Sciences, Maebashi, Gunma, Japan
[5]Department of Human and Information Sciences, School of Information Science and Technology, Tokai University, Hiratsuka, Kanagawa, Japan

Abstract

Neurofluids, a recently developed term that refers to interstitial fluids in the parenchyma and cerebrospinal fluid (CSF) in the ventricle and subarachnoid space, play a role in draining waste products from the brain. Neurofluids have been implicated in pathological conditions such as Alzheimer's disease and normal pressure hydrocephalus. Given that CSF moves faster in the CSF cavity than in the brain parenchyma, CSF motion can be detected by magnetic resonance imaging. CSF motion is synchronized to the heartbeat and respiratory cycle, but respiratory cycle-induced CSF motion has yet to be investigated in detail. Therefore, we analyzed CSF motion using dynamic improved motion-sensitized driven-equilibrium steady-state free precession-based analysis. We analyzed CSF motion linked to the respiratory cycle in four women and six men volunteers aged 23 to 38 years. We identified differences between free respiration and tasked respiratory cycle-associated CSF motion in the ventricles and subarachnoid space. Our results indicate that semi-quantitative analysis can be performed using the cranial site at which CSF motion is most prominent as a standard. Our findings may serve as a reference for elucidating the pathophysiology of diseases caused by abnormalities in neurofluids.

Keywords: cerebrospinal fluid, magnetic resonance imaging, respiratory cycle, neurofluids, dynamic improved motion-sensitized driven-equilibrium steady-state free precession

Introduction

In recent years, "neurofluids" has come into use as a general term for the interstitial fluids that perfuse the cerebral parenchyma as well as the cerebrospinal fluid (CSF) that moves through the ventricular

system and subarachnoid space.[1] Neurofluids are involved in the mutual exchange of substances that enter and exit the cerebral parenchyma across the vascular wall, thereby maintaining homeostasis of the central nervous system.[2,3] As solute clearance of substances such as amyloid beta occurs in tandem with the movement of neurofluids, the analysis of neurofluid dynamics may facilitate the diagnosis and treatment of Alzheimer's disease (AD).[4,5] Among neurofluids, dynamics of interstitial fluids have been studied in animal experiments using radioisotopes.[4] These tracers offer the best method of

studying the extremely slow movement of water molecules, which occurs on the order of several tens of micrometers per second.[6] However, these tracers require injection into the intracranial cavity, which is invasive and creates a non-physiological intracranial environment. Conversely, CSF moves rapidly within the subarachnoid space and ventricular system in the order of centimeters per second. Magnetic resonance imaging (MRI), a widely used non-invasive imaging modality, can thus be used to analyze CSF dynamics.[7]

CSF motion is underscored by two elements driven by respiration and heartbeat, respectively.[8–13] Heartbeat-driven CSF motion has been investigated in patients with idiopathic normal pressure hydrocephalus (iNPH) and AD.[14–17] However, the analysis of respiratory-driven CSF motion remains in the early stages of sequence development and assessment of analytical methods, and has not been harnessed to elucidate disease pathophysiology in patients.[13,18–20] In addition, most MRI-based analyses of respiratory-driven CSF motion have examined CSF in the spinal canal.[21–25] These studies have focused on cyclical changes in the venous circulation of the epidural space within the vertebral canal caused by changes in intrathoracic pressure and their relationship with CSF motion in the vertebral canal.

The objective of this study was to examine intracranial CSF dynamics associated with respiration in order to lay the foundation for investigating the pathophysiology of diseases such as iNPH and AD, which are more prevalent with advancing age. Given the decline in function of the respiratory and circulatory systems in humans with age, we analyzed respiratory-associated CSF motion, which has yet to be investigated in detail. This required the following MRI conditions: short scanning times, no trigger required to start scanning, capacity to observe several respiratory cycles, ability for the patient to start the respiratory task at any time, and compatibility with a range of MRI scanners. After exploring sequences that satisfied these requirements, we selected dynamic improved motion-sensitized driven-equilibrium steady-state free precession (iMSDE SSFP).[26,27]

With the ultimate goal of applying our dynamic iMSDE SSFP-based analysis of respiratory fluctuation-induced CSF motion in real-world clinical settings, this study aimed to: (1) determine the optimum sequence conditions in healthy volunteers, (2) perform observations during free respiration, (3) explore respiratory tasks that were not burdensome to participants, (4) identify whether the relationship between differences in respiratory tasks and cycles was accurately reflected, (5) identify differences between ventricle and subarachnoid space, and (6) perform a quantitative analysis of relevant parameters.

Materials and Methods

Participants

Participants consisted of ten healthy volunteers (four women and six men; aged 23–38 years). Young volunteers with normal cardiopulmonary function and no history of neurological, respiratory, or circulatory disease were enrolled. Following values express as mean ± standard deviation. Height was 165.8 ± 9.595 cm, weight was 57.50 ± 9.595 kg, and body mass index (BMI) was 20.91 ± 2.906 kg/m². This study received ethical approval from the internal review board of our institute (IRB No. 13R-066). All volunteers were enrolled after appropriate informed consent was obtained, consistent with the terms of our institutional internal review board's ethical standards.

Measurement of CSF motion

CSF motion was scanned during free-breathing and respiratory tasks in which participants inhaled and exhaled on either a 10 s (5 s for inspiration, followed by 5 s for expiration) or a 16 s (8 s for inspiration, followed by 8 s for expiration) cycle. Respiratory condition was monitored with a bellows pressure sensor placed on the participant's abdomen. Two-dimensional dynamic iMSDE SSFP was conducted with a 1.5 Tesla magnetic resonance (MR) scanner (Ingenia R5.3.1; Philips Healthcare, Best, The Netherlands) using a 15-channel receive-only dS Head Spine coil with velocity encoding (VENC) of 10 cm/s and motion-sensitized gradient direction of feet to head, anterior to posterior, and right to left. The following parameters were used: repetition time = 3.6 ms, echo time = 1.81 ms, flip angle = 60°, field of view = 250 mm, voxel size = 1.20 × 1.20 × 5 mm³, compressed sensing sensitivity encoding reduction factor = 2, dynamic scan time per slice = 413 ms, and dynamic scanning of 260 scans (scans up to number 40 were excluded and scans from numbers 41 to 260 were included). The associations between changes in intrathoracic pressure, respiration cycle, and MR signals were investigated.

Two respiration cycles were performed to explore breathing tasks that were not burdensome to participants. Participants were instructed to perform two respiratory tasks consisting of inhalation and exhalation for either 5 s or 8 s. The tasks were timed using a metronome at 1 beat per second, with the sound played every 5 s or 8 s to cue participants to switch between inhalation and exhalation. Concurrently, respiratory waveforms acquired by a respiratory

sensor were displayed on a console. Data from the real-time monitor screen and respiratory waveforms were recorded simultaneously using a video capture function. Both the respiratory sensor and video capture function were accessories to the MR unit.

To measure respiratory-driven CSF motion, midline sagittal sections were used as the scanning area, whereas the anterior horn of the lateral ventricle and the Sylvian fissure were scanned in oblique coronal sections. In sagittal sections, regions of interest (ROIs) were designated in the upper and lower parts of the fourth ventricle and anterior half of the third ventricle. In coronal sections, ROIs were designated in the Sylvian cistern and distal areas (outermost) of the Sylvian fissure close to the convexity of the subarachnoid space and anterior horn of the lateral ventricle.

Data analysis

Data analysis was conducted using MATLAB (R2020b; MathWorks, Natick, MA, USA). Changes in respiration and signal intensity during scanning were graphed using custom software developed by the authors. Signal intensities measured with dynamic iMSDE SSFP comprised relative numerical values. Intracycle signal intensities were integrated for analysis. The signal intensities acquired from individual participants varied widely, possible due to differences in the participants' physical properties, including tidal volume, cardiac stroke volume, abdominal pressure, and blood volume. To overcome this heterogeneity, the value from the 16-s cycle task at the upper part of the fourth ventricle during free breathing was used to normalize the differences in individual signal intensity and evaluate respiration-induced displacement of CSF. To quantify respiratory-induced variations in CSF motion, the time courses of dynamic iMSDE SSFP signal intensities in the ROIs at various anatomical locations were integrated for different respiratory conditions. The integrated values at all ROIs under all respiration conditions were then normalized using the value at the upper fourth ventricle in the 16-s respiration task based on the following equation:

$$\frac{\int_T S(t)\,dt}{\int_{T_{16}} S_{16,\ \text{IVth}}(t)\,dt} \times 100 \quad [\%]$$

where T_{16} is the observation time for the 16-s respiration task, $S_{16,\ \text{IVth}}(t)$ is the signal in the fourth ventricle for the 16-s task, and T and $S(t)$ are signals for an arbitrary anatomical location and respiratory condition.

Nonparametric analysis (Wilcoxon signed rank-sum test) was conducted to analyze the results for free-breathing and respiratory cycles. A p value <0.05 was considered statistically significant. All statistical data are presented as mean ± standard deviation.

Results

### Accuracy of respiration tasks

In a pilot study, repetitive cycles performed every 10 and 16 s were identified as feasible and acceptable breathing tasks for participants. Following values express as mean ± standard deviation. The respiration time of the ten participants was 3.62 ± 0.458 s during free respiration. The time required to perform the 10-s and 16-s cycle respiration tasks was 9.72 ± 0.775 s and 15.4 ± 1.43 s, respectively. No significant effects of height, weight, BMI, or sex of the participants on respiration task time were observed. Performance accuracy for the 10-s and 16-s respiration tasks was considered good.

MRI evaluation

Dynamic iMSDE SSFP was employed to measure respiratory task-coordinated signal changes in the Sylvian aqueduct, and above and below the foramen of Magendie (Fig. 1). In all participants, intensification of CSF motion in the cephalic direction during inspiration and in the caudal direction during expiration was observed in the third and fourth ventricles and cisterna magna. Signal changes unrelated to respiratory tasks were observed from the prepontine to premedullary cisterns and from the subarachnoid space on the anterior surface of the upper cervical cord. Wraparound artifacts (Fig. 1, arrow) were also evident. Signs resembling signal changes unrelated to respiratory tasks were observed in the superior sagittal sinus and deep cerebral veins under standard conditions (Fig. 1).

Relationship between respiratory sensors and MR signals

Examination of the relationship between bellows and MR signal changes revealed evident changes relative to free respiration (Fig. 2A and 2E) in the upper fourth ventricle when participants were engaged in a respiratory task (Fig. 2B). Signals were increased during expiration and were attenuated during inspiration. MR signals during the 16-s respiratory task are illustrated in Fig. 2B and 2D. The bellows and MR signals exhibited synchronization, with both plateauing at the changeovers between the expiratory and inspiratory phases. Close observation of the bellows and MR signal phases revealed that changes in MR signals lagged slightly behind those in the bellows (Fig. 2B and 2D).
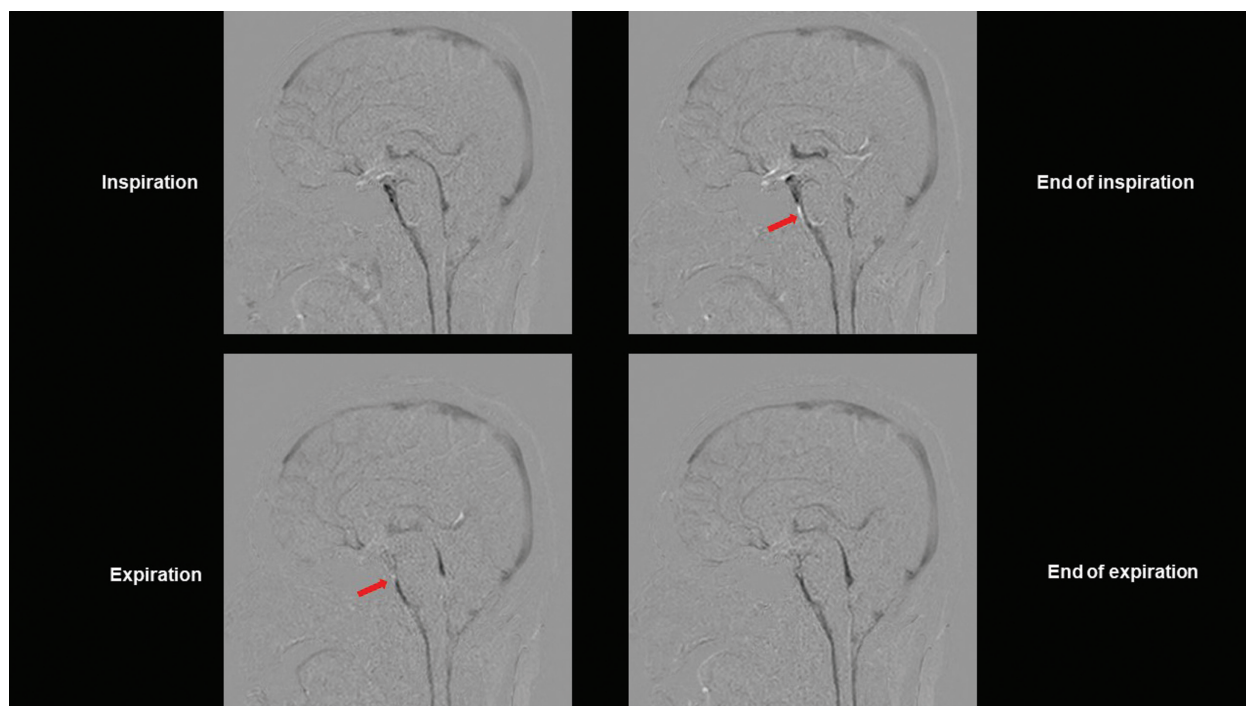
Fig. 1 Dynamic iMSDE SSFP images of an illustrative case. Dynamic iMSDE SSFP images of a 38-year-old women volunteer scanned in sagittal cross-section. The image with MSG off is subtracted from the image with MSG on. Areas of the scanned section in which movement is present are displayed as hypointense. The cerebral parenchyma is thus subtracted, and areas of the venous system in which perfusion is present are visualized as hypointense. Respiration-induced CSF motion in the fourth and third ventricles is visualized as hypointense. In the subarachnoid space at the anterior surface of the pons and medulla oblongata, turbulence due to CSF motion is apparent as a diminished MR signal. This site also reflects motion artifacts from movement of blood due to pulsation of the vertebral and basilar arteries. Due to concern that vascular motion artifacts may have interfered with analysis of CSF motion, an ROI was not designated at this site, and it was excluded from the analysis. Arrow: Wraparound artifact. iMSDE SSFP: improved motion-sensitized driven-equilibrium steady-state free precession, MSG: motion-sensitized gradient, CSF: cerebrospinal fluid, MR: magnetic resonance, ROI: region of interest

Differences were observed in MR signal changes between the upper fourth ventricle and distal Sylvian fissure, whereby MR signal changes in the distal Sylvian fissure were weaker than those in the upper fourth ventricle (p <0.05) (Fig. 2E). These effects were not intensified during performance of the respiratory tasks (Fig. 2F).

MR signal changes according to respiratory task and location

MR signal changes varied between participants and locations. Signal changes observed with dynamic iMSDE SSFP constituted relative numbers, and a comparative analysis was required for quantitative analysis of data for each participant and location based on these relative numbers. Therefore, signal changes in the upper fourth ventricle, the location exhibiting the greatest magnitude of signal changes, were used as reference values (Fig. 3) to enable normalization of individual differences.

To quantify the fluctuations in signal intensity, the integrated signal intensity ratio of a single respiratory cycle was calculated. Based on the assumption that the dynamic iMSDE SSFP signal would diminish with an increase in CSF velocity, the value of the integrated signal intensity ratio of a single respiratory cycle was considered to reflect the integral of this velocity, thereby constituting an expression of CSF displacement.

The value of the integrated signal intensity ratio of a single respiratory cycle decreased at each location from the 16-s cycle to the 10-s cycle, and from both cycles to free respiration (p <0.05) (Fig. 3). In the 16-s respiratory cycle, the integrated signal intensity ratio decreased in the ventricular system from the fourth ventricle to the third ventricle and subsequently to the lateral ventricle (p <0.05) (Fig. 3). However, no significant difference was observed between the upper and lower parts of the fourth ventricle (p = 0.114). In the subarachnoid space,
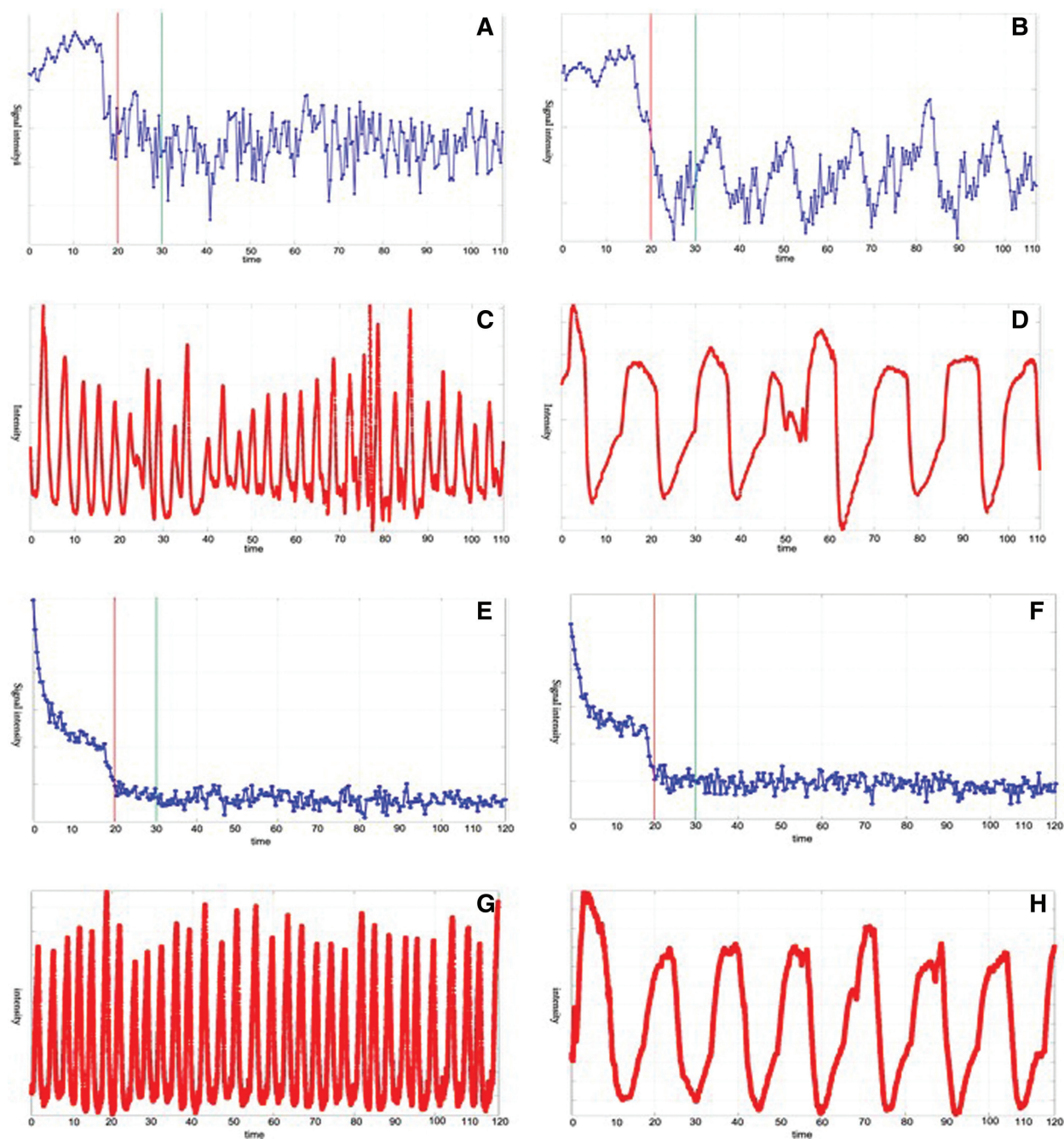
Fig. 2 MRI signal intensity changes and respiration cycle of an illustrative case. (A–D) Upper fourth ventricle. (E–H) Distal Sylvian fissure. (A, C, E, and G) Free breathing. (B, D, F, and H) 16-s cycle task. (A, B, E, and F) MR signal intensity changes due to CSF motion. The red lines in the images indicate the timing with MSG on. The signals after the green lines, when the signal had stabilized, were used in the analysis. The Y axis shows signal intensity in arbitrary unit. The X axis shows time in second. (C, D, G, and H) The participant's respiratory cycle, shown using data acquired with the bellows pressure sensor. The Y axis shows intensity in arbitrary unit. The X axis shows time in second. MRI: magnetic resonance imaging, MR: magnetic resonance, CSF: cerebrospinal fluid, MSG: motion-sensitized gradient

the integrated signal intensity ratio decreased from the Sylvian cistern to the distal part of the Sylvian fissure (p <0.05) (Fig. 3). In the third and fourth ventricles, the variance of the integrated signal intensity ratio tended to be greater during the 10-s task than during the 16-s task (p <0.05). These
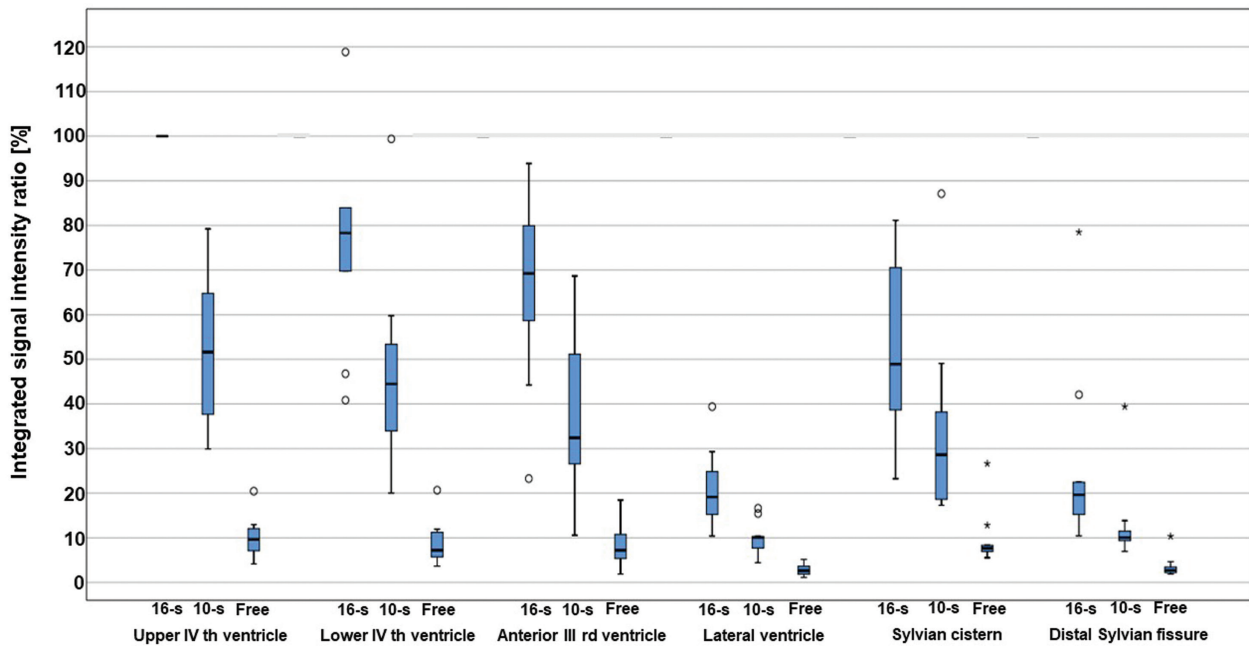
Fig. 3 Percentile changes of signal intensity in each region. Assuming that the value of the integrated signal intensity ratio of a single respiratory cycle MR signal decreases in accordance with CSF velocity, its integral therefore represents a quantity that corresponds to the integral of the velocity as an expression of CSF displacement. In the figure, values are expressed with reference to the lowest signal in the upper fourth ventricle, which is considered as 100%. The values are thus lower for free breathing, in which the signal changes are smaller. The following maximal extreme values (★) are not shown in this figure: 184% at the lower fourth ventricle, 148% at the anterior third ventricle, and 170% at the proximal Sylvian fissure. 10-s: 10-second cyclic task, 16-s: 16-second cyclic task, free: free-breathing, ○: outlier, ★: maximal extreme value, MR: magnetic resonance, CSF: cerebrospinal fluid.

results indicated that CSF displacement due to the respiratory task was more pronounced in the ventricular system than in the Sylvian fissure.
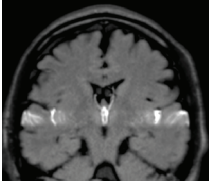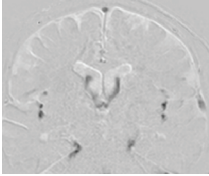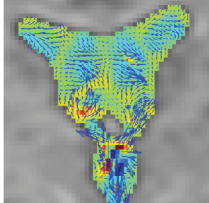
Discussion

Assessment of CSF motion using dynamic iMSDE SSFP provides a method of observing turbulence induced by the rapid CSF flow associated with the heartbeat.[26–28] In this study, dynamic iMSDE SSFP was applied to observe CSF motion synchronous with the respiratory cycle. Synchronized changes in CSF and components of the respiratory cycle were observed. These novel results were obtained despite short scan times, demonstrating that CSF motion was more strongly induced by respiratory tasks than by free respiration. Further, CSF motion was more strongly attenuated in the Sylvian fissure than in the ventricular system. Our findings highlight optimal respiratory task conditions that reflect differences in CSF motion induced by respiratory cycles and demonstrate that changes in displacement and velocity of CSF motion can be expressed as relative values by assigning a specific intracranial upper fourth ventricle as a reference.

The features of the time-resolved three-dimensional phase-contrast (PC) method, time-spatial labeling inversion pulse (time-SLIP) method, and dynamic iMSDE SSFP are summarized in Table 1. In the PC method, the MRI modality most commonly used to observe CSF motion, electrocardiography (ECG) or peripheral blood pulse waves are used triggers, and image acquisition is synchronized with the heartbeat. Given the short acquisition time due to the use of the heartbeat as a reference, this approach is unsuitable for use with respiration, which has a longer cycle. The time-SLIP method is another imaging modality used to assess CSF motion. This approach is capable of accurately expressing the motion of labeled CSF.[29] However, a labeling pulse must be applied to the CSF, and this method is limited by issues with timing, short acquisition time, and infeasible quantification.[6,18,30] Dynamic iMSDE SSFP does not require a trigger, is capable of measuring long cycles of CSF motion, and involves a short scanning time, thus enabling the observation of multiple respiratory cycles.[6,26,27] One limitation of

Table 1 Characteristics of CSF MRI sequences

Time-SLIP		Directly observes signal intensity changes due to transference of water protons from certain slab-like regions, in which proton spins are preexcited (by approximately 1–6 s).
Dynamic iMSDE SSFP		Detects and visualizes irregular movement of water protons as signal attenuation induced by phase dispersion in each voxel.
3DPC		Quantifies and visualizes time-resolved CSF velocity in 3D space, and thus enables characterization of CSF motion in a quantitative manner.

This table is based on Ref. 6 (*Neurol Med Chir (Tokyo)* 59: 133–146, 2019).
CSF: cerebrospinal fluid, MRI: magnetic resonance imaging, Time-SLIP: time-spatial labeling inversion pulse, iMSDE SSFP: improved motion-sensitized driven-equilibrium steady-state free precession, 3DPC: time-resolved three-dimensional phase contrast, 3D: three dimensional.

dynamic iMSDE SSFP is in pathophysiological evaluation, as it does not provide quantitative evaluation, similar to the time-SLIP method.[6,26] In the present study, MR signals were analyzed by integrating the signal changes over a single respiratory cycle to express CSF displacement and changes in CSF velocity induced by a respiratory task. This approach, which enabled the expression of the relationship between CSF velocity and a decrease in MR signal, may facilitate the elucidation of pathological conditions. Moreover, a comparison between different intracranial locations, in which one location was designated as the reference location, revealed that respiratory-driven CSF motion was suppressed on the lateral side of the Sylvian fissure compared with that in the ventricular system. This was consistent with the results obtained using the ECG-synchronized PC method, which could be due to suppression of the pressure gradient of the subarachnoid space by the arachnoid trabeculae. These results reflected the complex buffering effect of arachnoid trabeculae and vascular structures,[31] as previously discussed in the PC method.[8] Additionally, the outer border of the subarachnoid space is covered by the cranial vault, which limits pulsatile outward volume changes of the brain. Pulsatile inward brain volume changes would therefore result in enhancement of CSF displacement in the ventricular system.

Dynamic iMSDE SSFP measurement of changes in respiratory fluctuation-induced CSF motion revealed rapid changes in speed and spatial dispersion as decreases in signal intensity at locations where CSF passing through narrow tubular structures such as the Sylvian aqueduct and foramen of Magendie was ejected into wider spaces such as the cerebral ventricles. This phenomenon is also observed in cardiac-synchronized dynamic iMSDE SSFP,[26] and the changes in CSF motion driven by respiration and heartbeat are well explained in anatomical terms. However, unlike cardiac-driven changes, the signal changes in the third ventricle were smaller than those in the fourth ventricle, suggesting that the motive force supplied by respiration is transmitted from the lower part of the cranial cavity or side of the spinal canal.[21,25] It is well established that extensive transport of CSF occurs from the ventral surface of the brainstem to the upper cervical canal subarachnoid space.[8,26] This phenomenon was also observed in the present study. Wraparound artifacts[32] were also observed at this location. Enhanced signal intensity was noted in this area due to the location of the clivus at the ventral portion of the subarachnoid space and the long distance travelled by the

vertebrobasilar artery in this area. In the upper cervical spine, CSF motion may respond to changes in intrathoracic pressure by propagating upward, thereby enhancing CSF motion, with both arterial and respiratory elements complementing each other. Despite adjusting the MR sequence with VENC, the details of respiratory-driven CSF motion at this location were difficult to ascertain, which was a limitation of the present study.

In the intracranial space, CSF moved in the cephalic direction during inspiration and in the opposite (caudal) direction during expiration. This association between the direction of CSF motion and the respiratory cycle is well established[18,19] and is underscored by the Monro–Kellie theory.[22,33] With regard to the relationship between respiratory fluctuations and CSF motion, Vinje et al. reported notable findings from overnight pressure monitoring via a catheter and MRI of patients with iNPH.[12] In the present study, synchronous recordings of MRI signals and a bellows pressure sensor fitted to the abdominal wall were performed while participants were inside the MR scanner. These simultaneous recordings underscored the need to pay attention to the time lag between changes in intrathoracic pressure and their transmission as abdominal wall movements, as well as the time difference between changes in intrathoracic pressure and their transmission to the CSF via structures such as the epidural venous plexus. With regard to the use of respiratory tasks, small changes in CSF motion during free respiration were noted, but CSF motion was intensified by the imposition of a respiratory task, which complements Vinje et al.'s[12] conclusion that pressure gradients "induce CSF flow volumes dominated by respiration." These findings are also consistent with other reports indicating that respiratory-driven CSF motion is induced by tasks including deep breathing and breath-holding,[18,21] hyperventilation,[13] and coughing.[34] However, the present method induced appreciable changes in CSF motion despite employing repeated slow respiratory cycles. A comparison of the 16-s and 10-s tasks revealed that the variance of the integral value in the fourth and third ventricles tended to be lower in the 16-s task than in the 10-s task, suggesting that the task with the shorter cycle may have induced smaller respiratory fluctuations. In this regard, short respiration cycles may have resulted in insufficient changes in MR signals.

Future directions

In CSF displacement, CSF motion driven by respiratory fluctuations is considered more important than that driven by the heartbeat.[9–11] The transmission of respiratory fluctuations to CSF is of interest for the transportation of substances in the cerebral ventricles, in which CSF can move freely in the absence of barriers such as the arachnoid trabeculae. The results presented herein may facilitate the elucidation of neurofluid dynamics and pathophysiology of AD and iNPH following solute clearance from the vascular walls or cerebral parenchyma and subsequent movement to the subarachnoid space or cerebral ventricles. The current findings may also be applicable for investigating the dynamics of CSF and blood in blood vessels when examining the association between age-related cardiopulmonary functional decline and neurological function.

Study limitations

This study has several limitations. One limitation was the age distribution of volunteers. Relatively young individuals were selected as volunteers, and future studies should collect data from individuals in mid-life to old age. Another limitation was the accuracy of tidal volume measurements. To evaluate the relationship between respiratory cycle and CSF motion with greater accuracy, the use of a spirometer or similar device for the quantitative measurement of single tidal volume should be considered, provided that this does not impose a burden on subjects or cause ethical issues.

Conclusions

A procedure for observing respiratory cycle-induced changes in CSF motion in healthy individuals was developed using dynamic iMSDE SSFP. This approach enabled semi-quantitative identification of CSF dynamics in the cranial cavity in response to respiratory cycle changes. In addition to previous cardiac-synchronized methods, a respiratory-synchronized CSF motion mechanism was presented, which may provide insight into the pathophysiology of neurofluid-associated diseases.

Acknowledgments

Conflicts of Interest Disclosure

The authors declare no conflicts of interest.

References

1) Agarwal N, Contarino C, Toro E: Neurofluids: a histolic approach to their physiology, interactive dynamics and clinical implications for neurological diseases. *Veins Lymphat* 8: 49, 2019

2) Matsumae M, Sato O, Hirayama A, et al.: Research into the physiology of cerebrospinal fluid reaches a new horizon: intimate exchange between cerebrospinal fluid and interstitial fluid may contribute to maintenance of homeostasis in the central nervous system. *Neurol Med Chir (Tokyo)* 56: 416–441, 2016

3) Bakker EN, Bacskai BJ, Arbel-Ornath M, et al.: Lymphatic clearance of the brain: perivascular, paravascular and significance for neurodegenerative diseases. *Cell Mol Neurobiol* 36: 181–194, 2016

4) Carare RO, Teeling JL, Hawkes CA, et al.: Immune complex formation impairs the elimination of solutes from the brain: implications for immunotherapy in Alzheimer's disease. *Acta Neuropathol Commun* 1: 48, 2013

5) Tarasoff-Conway JM, Carare RO, Osorio RS, et al.: Clearance systems in the brain-implications for Alzheimer disease. *Nat Rev Neurol* 11: 457–470, 2015

6) Matsumae M, Kuroda K, Yatsushiro S, et al.: Changing the currently held concept of cerebrospinal fluid dynamics based on shared findings of cerebrospinal fluid motion in the cranial cavity using various types of magnetic resonance imaging techniques. *Neurol Med Chir (Tokyo)* 59: 133–146, 2019

7) Jaeger E, Sonnabend K, Schaarschmidt F, Maintz D, Weiss K, Bunck AC: Compressed-sensing accelerated 4D flow MRI of cerebrospinal fluid dynamics. *Fluids Barriers CNS* 17: 43, 2020

8) Matsumae M, Hirayama A, Atsumi H, Yatsushiro S, Kuroda K: Velocity and pressure gradients of cerebrospinal fluid assessed with magnetic resonance imaging. *J Neurosurg* 120: 218–227, 2014

9) Takizawa K, Matsumae M, Sunohara S, Yatsushiro S, Kuroda K: Characterization of cardiac- and respiratory-driven cerebrospinal fluid motion based on asynchronous phase-contrast magnetic resonance imaging in volunteers. *Fluids Barriers CNS* 14: 25, 2017

10) Yatsushiro S, Sunohara S, Takizawa K, Matsumae M, Kajihara N, Kuroda K: Characterization of cardiac- and respiratory-driven cerebrospinal fluid motions using correlation mapping with asynchronous 2-dimensional phase contrast technique. Conference proceedings: Annual International Conference of the IEEE Engineering in Medicine and Biology Society 2016: p3867–p3870, 2016

11) Yatsushiro S, Sunohara S, Tokushima T, et al.: Characterization of cardiac- and respiratory-driven cerebrospinal fluid motions using a correlation mapping technique based on asynchronous two-dimensional phase contrast MR imaging. *Magn Reson Med Sci* Feb 6, 2021, ahead of print

12) Vinje V, Ringstad G, Lindstrøm EK, et al.: Respiratory influence on cerebrospinal fluid flow - a computational study based on long-term intracranial pressure measurements. *Sci Rep* 9: 9732, 2019

13) Chen L, Beckett A, Verma A, Feinberg DA: Dynamics of respiratory and cardiac CSF motion revealed with real-time simultaneous multi-slice EPI velocity phase contrast imaging. *Neuroimage* 122: 281–287, 2015

14) Takizawa K, Matsumae M, Hayashi N, Hirayama A, Yatsushiro S, Kuroda K: Hyperdynamic CSF motion profiles found in idiopathic normal pressure hydrocephalus and Alzheimer's disease assessed by fluid mechanics derived from magnetic resonance images. *Fluids Barriers CNS* 14: 29, 2017

15) Han F, Chen J, Belkin-Rosen A, et al.: Reduced coupling between cerebrospinal fluid flow and global brain activity is linked to Alzheimer disease-related pathology. *PLoS Biol* 19: e3001233, 2021

16) He WJ, Zhou X, Long J, et al.: Idiopathic normal pressure hydrocephalus and elderly acquired hydrocephalus: evaluation with cerebrospinal fluid flow and ventricular volume parameters. *Front Aging Neurosci* 12: 584842, 2020

17) Tawfik AM, Elsorogy L, Abdelghaffar R, Naby AA, Elmenshawi I: Phase-contrast MRI CSF flow measurements for the diagnosis of normal-pressure hydrocephalus: observer agreement of velocity versus volume parameters. *AJR Am J Roentgenol* 208: 838–843, 2017

18) Yamada S, Miyazaki M, Yamashita Y, et al.: Influence of respiration on cerebrospinal fluid movement using magnetic resonance spin labeling. *Fluids Barriers CNS* 10: 36, 2013

19) Spijkerman JM, Geurts LJ, Siero JCW, Hendrikse J, Luijten PR, Zwanenburg JJM: Phase contrast MRI measurements of net cerebrospinal fluid flow through the cerebral aqueduct are confounded by respiration. *J Magn Reson Imaging* 49: 433–444, 2019

20) Schroth G, Klose U: Cerebrospinal fluid flow. II. Physiology of respiration-related pulsations. *Neuroradiology* 35: 10–15, 1992

21) Dreha-Kulaczewski S, Joseph AA, Merboldt KD, Ludwig HC, Gärtner J, Frahm J: Inspiration is the major regulator of human CSF flow. *J Neurosci* 35: 2485–2491, 2015

22) Lloyd RA, Butler JE, Gandevia SC, et al.: Respiratory cerebrospinal fluid flow is driven by the thoracic and lumbar spinal pressures. *J Physiol* 598: 5789–5805, 2020

23) Peters K, Weiss K, Maintz D, Giese D: Influence of respiration-induced B0 variations in real-time phase-contrast echo planar imaging of the cervical cerebrospinal fluid. *Magn Reson Med* 82: 647–657, 2019

24) Aktas G, Kollmeier JM, Joseph AA, et al.: Spinal CSF flow in response to forced thoracic and abdominal respiration. *Fluids Barriers CNS* 16: 10, 2019

25) Dreha-Kulaczewski S, Konopka M, Joseph AA, et al.: Respiration and the watershed of spinal CSF flow in humans. *Sci Rep* 8: 5594, 2018

26) Horie T, Kajihara N, Matsumae M, et al.: Magnetic resonance imaging technique for visualization of irregular cerebrospinal fluid motion in the ventricular

system and subarachnoid space. *World Neurosurg* 97: 523–531, 2017

27) Horie T, Kajihara N, Saito H, et al.: Visualization of cerebrospinal fluid motion in the whole brain using three-dimensional dynamic improved motion-sensitized driven-equilibrium steady-state free precession. *Magn Reson Med Sci* 20: 112–118, 2021

28) Atsumi H, Horie T, Kajihara N, Sunaga A, Sakakibara Y, Matsumae M: Simple identification of cerebrospinal fluid turbulent motion using a dynamic improved motion-sensitized driven-equilibrium steady-state free precession method applied to various types of cerebrospinal fluid motion disturbance. *Neurol Med Chir (Tokyo)* 60: 30–36, 2020

29) Yamada S, Miyazaki M, Kanazawa H, et al.: Visualization of cerebrospinal fluid movement with spin labeling at MR imaging: preliminary results in normal and pathophysiologic conditions. *Radiology* 249: 644–652, 2008

30) Shibukawa S, Miyati T, Niwa T, et al.: Time-spatial labeling inversion pulse (Time-SLIP) with pencil beam pulse: a selective labeling technique for observing cerebrospinal fluid flow dynamics. *Magn Reson Med Sci* 17: 259–264, 2018

31) Yaşargil MG: Microsurgical Anatomy of the Basal Cisterns and Vessels of the Brain, Diagnostic Studies, General Operative Techniques and Pathological Considerations of the Intracranial Aneurysms. New York, Georg Thieme Verlag, 1984

32) Chen K, Niu F, Zou H, Lu J: Modification of frequency-domain active noise control algorithm without secondary path modeling. *J Acoust Soc Am* 149: 1021, 2021

33) Delaidelli A, Moiraghi A: Respiration: a new mechanism for CSF circulation? *J Neurosci* 37: 7076–7078, 2017

34) Yildiz S, Thyagaraj S, Jin N, et al.: Quantifying the influence of respiration and cardiac pulsations on cerebrospinal fluid dynamics using real-time phase-contrast MRI. *J Magn Reson Imaging* 46: 431–439, 2017

Corresponding author: Mitsunori Matsumae, MD, PhD
Department of Neurosurgery, Tokai University School of Medicine, 143 Shimokasuya, Isehara, Kanagawa 259-1193, Japan.
e-mail: mike@is.icc.u-tokai.ac.jp